22nd International Conference on Renewable Energies and Power Quality (ICREPQ'24)
Bilbao (Spain), 26th to 28th June 2024
Renewable Energy and Power Quality Journal (RE&PQJ)
ISSN 2172-038 X, Volume No.22, September 2024

Speech Measurement Delay and its Influence on IFOC Tuning

F. Barrero[1], M.G. Satué[2] and F. Colodro[1]

[1] Department of Electronic Engineering
[2] Department of System and Automation Engineering
E.T.S.I., University of Sevilla
Camino de los Descubrimientos sn, 41092 Sevilla (Spain)
Phone/Fax number: +0034 954 487372

Abstract. The Indirect Field-Oriented Control technique has been in use since the 1960s, with some innovations added to the basic original setting. Although variable-speed drive technology has evolved considerably, basic assumptions remain in place. This paper deals with the problem of sensing the mechanical speed using optical devices. This aspect has not been considered in previous works. To focus the contribution, finite-state model predictive control is used in this paper for stator current control. The outer (speed) loop considers PI control as is usually the case. The experimental results presented here show the need for new tuning methods.

Keywords. Application of power electronics, Digital implementation, Mechanical and aerospace estimation, Quantized systems, Real-time control, Tuning.

1. Introduction

Indirect Field Oriented Control (IFOC) is, as of today, a popular method for Induction Motor (IM) speed control which is used not only in academia but also in industrial applications under various denominations such as vector control. The method typically uses PI controllers for the speed loop and the inner current loops. More recently, proposals such as Finite State Model Predictive Control (FSMPC) replace inner loops with a model-based method capable of performing direct digital control of the voltage source inverter (VSI) as in [1]. In this way, the Pulse Width Modulation (PWM) stage can be eliminated with an increase in the system performance as reported in [2].

Regarding PI tuning for IFOC, influential works of the 1990s and early 2000s provide tuning methods where global stability is guaranteed under some, not quite stringent, requirement of knowing the rotor time constant of the IM [3]–[6]. At the core of these methods, a dynamic model of the current-fed IM is used. Often, the models used do not consider some practical issues. Among these, one can encounter nonlinearities in the IM dynamics, VSI+modulation behavior, and aspects derived from the use of a Digital Signal Processor (DSP) for the PI+IFOC algorithms.

In the following 20 years, some papers have appeared that expand the previous works in various manners. Most of the efforts have concentrated on sensorless operation, estimation of the rotor time constant, extension of the PI with operating-point based scheduling and/or adaptivity, fault-tolerant capabilities, and finally tuning methods based on extensive simulation/experimentation. Also, many contending technologies have been proposed to replace the speed PI. Despite all of this, conventional PI control is still reported as competitive due to its simple implementation compared to nonlinear control [7]–[8], adaptive control [9]–[10], robust control [11], and some exotic fuzzy and/or neural approaches [12]–[13]. The experimental approach has been used for PI tuning as a means of coping with the lack of theoretical models to analyze the above cited practical aspects and their influence on complex figures of merit such as the Integral Time-multiplied Absolute Error (ITAE). For example, the work in [14] uses metaheuristic optimization algorithms for optimal tuning of the PI.

In addition to the above, in recent years, more complex drives have been the subject of research. These use machines other than conventional three-phase IM and/or converters other than the two-level three-phase one [15]. Many new systems include multiphase IM, multilevel VSI, and others [16]. The multiphase case is especially interesting for this study as the overall structure of the controller is IFOC-like. The tuning of the inner-loop PIs is more complex due to the interaction among phases. In particular, the existence (in multiphase IM stator currents) of a torque producing plane (α−β) and various harmonic planes (x_j−y_j with j≥1) makes the control design more challenging. For instance, modulation schemes for 6 and 5-phase drives have little to do with each other, yet predictive controllers have the same structure for both. Also, multiphase drives require at least four PI controllers for the PWM method and just one predictive controller for FSMPC. So, FSMPC has made the problem more tractable but at the cost of increased computational needs [17]. These needs are nowadays covered by modern DSP, especially with the very recent advent of non-iterative solutions [18]. Also, the FSMPC method is becoming popular for its flexibility. For example, modulation variants that are impossible with PWM can be used with FSMPC [19]–[20], the mechanical load characteristics can be considered with ease [21], and fault tolerance capabilities are better utilized [22]. On the other hand, simple tuning rules are no longer applicable [23]–[24].

In this context, the authors believe that some particular aspects derived from the DSP implementation of IFOC-like methods must be investigated. Note that this question has been raised in the past. For example, [6] was concerned about "...technological effects of sampling and PWM synthesis in the implementation of the control law". In this context, the work in [25] relies on a better predictive model that includes digital control and PWM delays. The time delays are accounted for by reference augmentation obtained through an integrator. However, the PI tuning is not considered. In this paper, the PWM is replaced by a predictive approach that features a higher bandwidth compared to PWM. Regarding sampling, this paper considers the velocity estimation problem [26]. The present-day device and the common method for velocity estimation are considered, and their relationship with PI tuning is exposed by means of experimentation. Note that velocity estimation directly affects the speed regulation loop and indirectly the inner loop, as measured speed is used in the calculation of the flux angle [27] and the predictive model coefficients [1]. Since this paper is focused on experimentation, a particular IFOC-like structure must be considered. This corresponds to a 5-phase IM where the inner control loop is performed using FSMPC.

2. IFOC Structure used in the Experiments

In the indirect field-oriented control scheme, flux and torque are independently regulated. The flux current set point i_d^* is set to magnetize the motor whereas quadrature current i_q^* is used to manipulate the produced torque. The PI in the velocity feedback loop is responsible for generating i_q^* to drive the mechanical speed control error to zero.

$$i_q^* = k_p \cdot e + k_i \cdot \int_0^\infty e(\tau)d\tau \qquad (1)$$

where $e = \omega^* - \omega_m$ is the velocity error or difference between the speed set point (ω^*) and the measurement of the mechanical speed (ω_m).

Once the set points in the d−q coordinates are known, they are projected to the α−β space using the Park transformation, obtaining a reference for the stator current in α−β plane as $I_{\alpha-\beta}^* = \mathrm{D}\left(i_d^*, i_q^*\right)^T$, where matrix D is given by

$$\mathrm{D}=\begin{pmatrix} \cos\theta_e & \sin\theta_e \\ -\sin\theta_e & \cos\theta_e \end{pmatrix} \qquad (2)$$

The flux position θ_e is estimated as $\theta_e = \int \omega_e\, dt$, where $\omega_e = \omega_{sl} + P \cdot \omega_m$, being P the number of pairs of poles of the IM and the slip frequency:

$$\omega_{sl} = \frac{i_q^*}{i_d^*} \cdot \frac{1}{\hat{\tau}_r} \qquad (3)$$

where $\hat{\tau}_r$ is an estimation of the rotor time constant $\frac{L_r}{R_r}$, being L_r and R_r the inductance and the resistance of the rotor, respectively. As a result, the set point for stator current tracking $i^*(k)$ has an amplitude $I^* = \sqrt{i_d^{*\,2} + i_q^{*\,2}}$. Finally, the stator current references can be expressed as $i_\alpha^*(t) = I^* sin\omega_e t$, $i_\beta^*(t) = I^* cos\omega_e t$, $i_x^*(t) = 0$, $i_y^*(t) = 0$. Note that a distributed winding multiphase IM is considered.

A. FSMPC Control of a 5-phase IM

The inner loop of an IFOC scheme is responsible for producing stator currents in α−β that follow their references and, at the same time, maintaining x−y currents close to zero, as they do not produce torque but contribute to losses. This task can be accomplished using the FSMPC strategy. A model of the IM is needed to predict the IM behavior for each possible VSI configuration. Using the vector space decomposition, the 5-phase stator currents are projected in the energy conversion plane (α−β), the harmonic plane (x−y) and the homopolar component z, resulting in equations relating stator voltages, $v_s(t)$, stator and rotor currents, $i_s(t)$ and $i_r(t)$, fluxes, $\psi_s(t)$ and $\psi_r(t)$, and rotor electrical angular speed $\omega_r(t) = P \cdot \omega_m(t)$ as follows:

$$\begin{aligned} v_{\alpha\beta s}(t) &= R_s\, i_{\alpha\beta s}(t) + p\psi_{\alpha\beta s}(t) \\ 0 &= R_r\, i_{\alpha\beta r}(t) + p\psi_{\alpha\beta r}(t) - j\omega_r(t)\psi_{\alpha\beta r}(t) \\ \psi_{\alpha\beta s}(t) &= L_s\, i_{\alpha\beta s}(t) + L_m\, i_{\alpha\beta r}(t) \\ \psi_{\alpha\beta r}(t) &= L_m\, i_{\alpha\beta s}(t) + L_r\, i_{\alpha\beta r}(t) \\ v_{xyzs}(t) &= R_s\, i_{xyzs}(t) + p\psi_{xyzs}(t) \\ \psi_{xyzs}(t) &= L_{ls}\, i_{xyzs}(t) \end{aligned} \qquad (4)$$

where p is the derivative operator, and the following machine parameters are used: resistances R_s, R_r, inductances L_s, L_r, leakage inductance L_{ls} and mutual inductance L_m. Sub-index s stands for stator and r for rotor. Stator voltages are produced by VSI according to the gating signals K_j for the VSI legs j=1, ..., 5 accommodated in u=(K_1, ..., K_5) ∈ B^5 with B={0,1}. The resulting voltages $v_{\alpha\beta xyzs}$ are

$$v_{\alpha\beta xyzs} = \left(v_{\alpha s}, v_{\beta s}, v_{xs}, v_{ys}, v_{zs}\right) = \tfrac{2}{25} V_{DC}\mathbf{TM}u \qquad (5)$$

where V_{DC} is the DC link voltage, **T** is a connectivity matrix that keeps invariant the original values of the electrical variables after the transformation but not the total powers, and **M** is a coordinate transformation matrix accounting for the spatial distribution of machine windings.

$$\mathbf{TM} = \begin{pmatrix} d & \gamma_1^c & \gamma_2^c & \gamma_3^c & \gamma_4^c \\ 0 & \gamma_1^s & \gamma_2^s & \gamma_3^s & \gamma_4^s \\ d & \gamma_2^c & \gamma_4^c & \gamma_6^c & \gamma_8^c \\ 0 & \gamma_2^s & \gamma_4^s & \gamma_6^s & \gamma_8^s \\ c & c & c & c & c \end{pmatrix} \begin{pmatrix} a & b & b & b & b \\ b & a & b & b & b \\ b & b & a & b & b \\ b & b & b & a & b \\ b & b & b & b & a \end{pmatrix} \qquad (6)$$

The coefficients used are: $a = 4, b = -1, c = 1/2, d = 1$, $\gamma_h^c = cosh\vartheta, \gamma_h^s = sinh\vartheta, \vartheta = 2\pi/5$ for the five phase IM. The actual values of the electrical parameters corresponding to the machine used in the experiments are given in Table I.

Table I. - Parameters of the five-phase IM

Parameter	Value	Unit
Stator resistance, R_s	12.85	Ω
Rotor resistance, R_r	4.80	Ω
Stator leakage inductance, L_{ls}	79.93	mH
Rotor leakage inductance, L_{lr}	79.93	mH
Mutual inductance, L_m	681.7	mH
Rotational inertia, J_m	0.02	kg m^2
Number of pairs of poles, P	3	-

In discrete time k, the control action $u(k+1)$ is computed minimizing a cost function J. The cost function penalizes the stator currents tracking error as $J = \|i^*(k+2) - \hat{\imath}(k+2)\|^2$, where $\hat{\imath}(k+2)$ are the predicted currents. Note the one sampling period delay due to computations.

The developed electrical torque is derived from the actual values of the direct and quadrature stator currents as

$$T_e = \frac{5}{2} P \frac{L_m^2}{L_{lr}+L_m} \cdot i_d i_q \qquad (7)$$

B. Mechanical speed estimation

In many applications, the mechanical speed is obtained from an optical sensor that provides a train of pulses as the axis rotates. Typical optical devices can produce a few thousand pulses per revolution (ppr). Additionally, DSP often provides routines for encoder pulse treatment, such as the eQEP module of the TMS320F28335. This peripheral obtains the quadrature pulses from which it infers the rotation direction and the number of pulses arriving. The conventional method for speed estimation uses the pulse count for a certain time period T_ω. A fixed-time interruption of the eQEP is used to ensure a constant T_ω value. The number of pulses that arrive since the last interruption Q_ω is then used to estimate the angular velocity as

$$\omega_e = K_\theta \frac{Q_\omega}{T_\omega} \qquad (8)$$

where K_θ(rad/ppr) is a parameter of the optical sensor. It is computed as the ratio $2\pi/P_r$, where P_r is the number of pulses per revolution. In the experiments, a GHM510296R/2500 encoder is used, providing $P_r = 10^4$ ppr.

The conventional method provides reasonable speed estimates except in the low-speed range, where Q_ω does not represent a good average. In this case an erratic behavior of the estimated speed is observed as analyzed in [26]. Longer values for T_ω would be required, but this makes the estimation to lag behind the actual speed, so a trade-off solution must be established.

In addition to the conventional method, there are others, more sophisticate, that seek to eliminate the above problems, as in [28]. However, these are not commonly found. At any rate, and for the purposes of this paper, the conventional method is a good starting point.

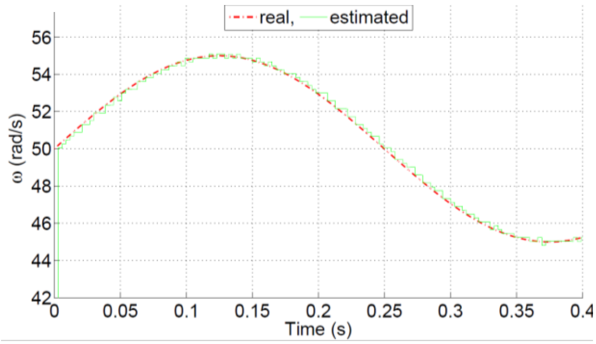

Fig. 1. Mechanical speed and its estimation using the conventional method with $\boldsymbol{T_\omega} = \mathbf{3}$ ms.

A model for the speed measurement process can be estimated from (8) considering that the arrival times of pulses is linked to the actual speed. In practice the simple model $\omega_e(t) = \omega(t - T_\omega)$ is found to provide a good match. This model neglects steady state deviations of speed measurements and treats the measurement process as a time delay. Figure 1 shows a simulation of the method using fixed-time interruption with $T_\omega = 3$ ms, which is a value commonly found. In said Fig. 1, the actual speed has been set to follow a sinusoidal trajectory around a base value of 50 rad/s. Measurements are taken at the FSMPC sample rate asynchronously with the EQEP interruption. It can be appreciated that the ω_e values are updated at intervals of $T_\omega = 3$ ms.

C. Other experimental issues

In addition to the mechanical speed estimation problem, IFOC-like structures must face other problems. Among this, one can encounter:

- Intrinsic nonlinearities in the system such as saturation of currents.
- Delays due to modulation.
- Detuning of IFOC due to parameter excursions.

These phenomena are present in experimentation, and PI tuning must cope with them.

3. Experiments

The PI tuning is assessed in this section by means of tests in the experimental setup described below.

A. Laboratory Setup

The laboratory arrangement depicted in Fig. 2 is used. A five-phase motor with parameters shown in Table I is powered by a five-phase VSI constructed from two three-phase SEMIKRON SKS 22F modules. A 300V DC power supply is used in the DC-link. The control programs run on a MSK28335 board housing a TMS320F28335 DSP. Hall effect sensors (LH25-NP) are used to measure the stator phase currents. Last, a DC motor is used sharing the same shaft as the IM to provide an opposing torque load (T_L) for the tests.

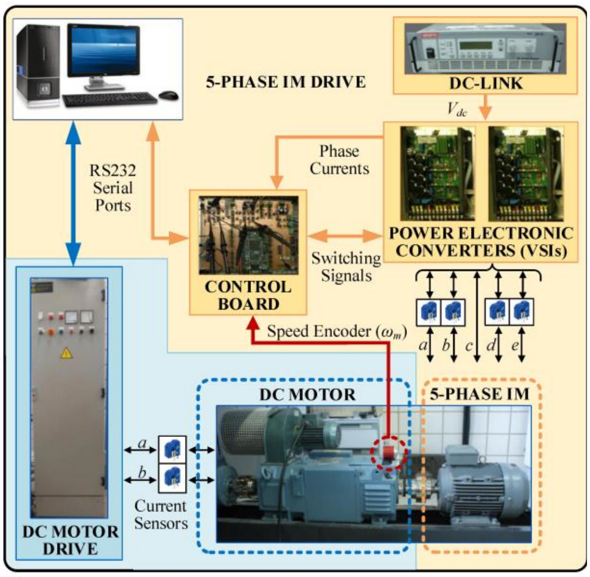

Fig. 2. Diagram and photographs of the laboratory setup used in the experiments.

Table II. - PI Tunings Used in the Experiments

	PI Gains		Ideal performance	
ID	$k_p \cdot 10^3$	$k_i \cdot 10^5$	*PO* (%)	T_r (s)
T1	80	70	4.4	0.149
T2	72	16	7.7	0.151

Table III. - Experimental Results

ID	*PO* (%)	T_r (s)	R_T (Nm)	ITAE
T1	4.21	0.171	0.0281	540
T2	6.57	0.174	0.0278	25
$T2^d$	6.02	0.250	0.0254	55

B. PI Tuning

According to [6], the PI tuning for IFOC can be performed by placing the closed loop poles, from which the coefficients of a degree-two Hurwitz polynomial can be determined. Said coefficients are linked to the k_p and k_i PI gains. In principle, and for a wide range of detuned systems (i.e. values of $k = \frac{\tau_r}{\hat{\tau}_r}$ other than 1), the closed loop damping and natural frequency can be obtained by PI tuning using some equations (see eq. (11) in [29]).

The PI gains used in the experiments and their expected performance are provided in Table II, where *PO* is the percentage overshoot and T_r is the rise time for a step test. T1 tuning is the theoretical tuning to obtain a small overshoot and acceptable rise time (these values are application dependent, of course). Note that this tuning does not consider effects such as the mechanical speed estimation process. The T2 tuning is more conservative, providing diminished performance (although still acceptable for many applications).

C. Obtained results

The experimental setup is now used to obtain the actual performance of the considered PI tunings. Experiments consist of step tests, starting with zero speed. The final value for the reference speed is 500 rpm. For these experiments, the *PO* and T_r are recorded.

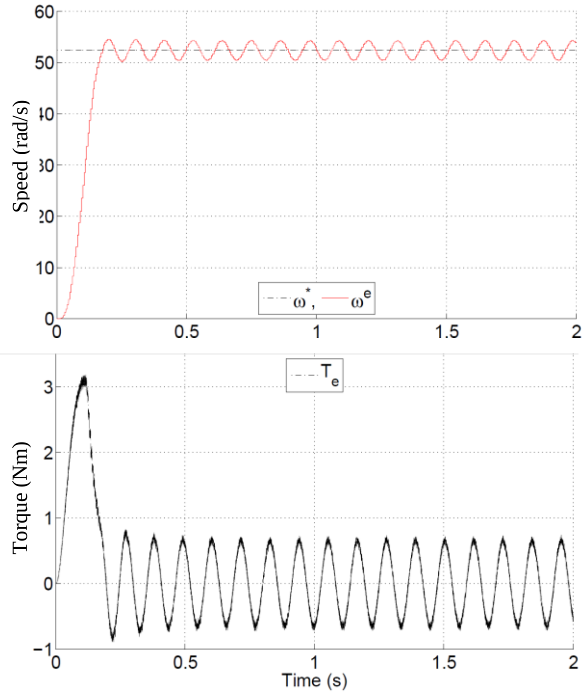

Fig. 3. Trajectories of speed (top) and torque (bottom) for a step test using tuning T1.

Two more figures of merit are added. The first one is the torque ripple, defined as

$$R_T = \sqrt{\frac{1}{N}\sum_{k=1}^{N}(T^*(k) - T(k))^2} \qquad (9)$$

where the reference value T^* is obtained from (7) using the reference values for stator currents. The torque ripple must be kept within limits as it can produce damage to the drive in the long run.

The second added figure of merit is the ITAE, defined for discrete time as

$$ITAE = \frac{1}{N}\sum_{k=1}^{N}\frac{\|\omega^*(k)-\omega(k)\|}{\omega^*(k)}k \qquad (10)$$

The first tuning (T1) produces the results shown in Fig. 3 and in Table III. It can be seen that the performance has degraded relative to the expected values presented in Table II. More importantly, the behavior of the speed is too oscillatory, showing poor damping. Alternate tuning is found by simply reducing the PI gains. This produces tuning T2, whose performance is shown in Fig. 4. With this tuning, the closed loop response is more adequate, without the persisting oscillations of the previous case. As a result, the *ITAE* value is much lower. However, this comes at the price of another degradation of the merit figures, as shown in Table III. Finally, the entry marked $T2^d$ represents the tuning T2, but for a purposely detuned system in which k=1.45. For this experiment, the DSP program realizing the PI, IFOC and FSMPC computations are given detuned values of R_r and L_m. As a result, the response to the step

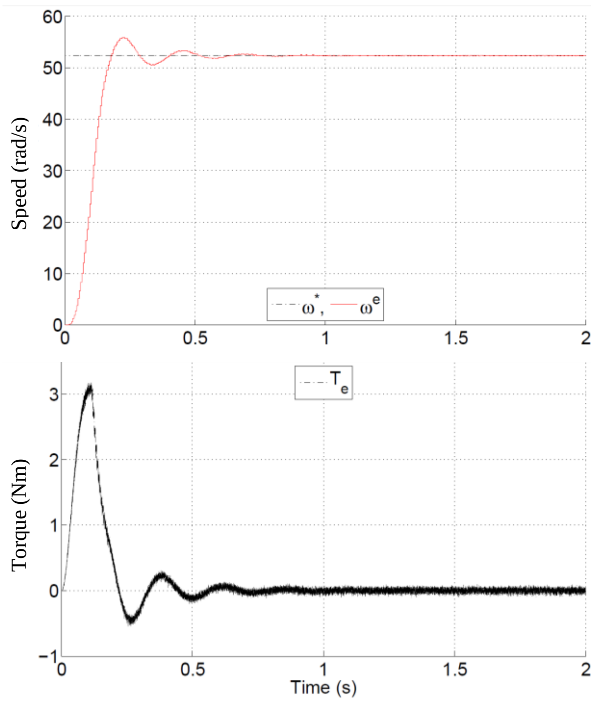

Fig. 4. Trajectories of speed (top) and torque (bottom) for a step test using tuning T2.

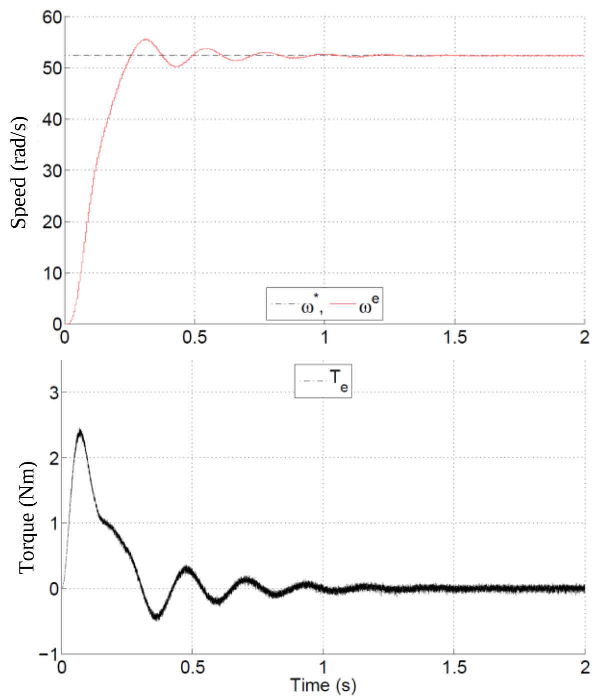

Fig. 5. Trajectories of speed (top) and torque (bottom) for a step test using tuning T2[d].

test degrades, as can be seen in Fig. 5 and Table III. Rise time and *ITAE* are the most affected figures of merit.

4. Conclusion

The effect of speed measurement on PI tuning has been explored. The main result is that, coupled with rotor time constant detuning, the measurement process degrades the expected performance. In particular, the ITAE is seriously affected, prompting for a reevaluation of the models and methods used for PI tuning.

Acknowledgement

This work is part of the Grant TED2021-129558B-C22 funded by MCIN/AEI/10.13039/501100011033 and by the “European Union NextGenerationEU/PRTR”. Also, the authors want to thank the support provided by project I+D+i/PID2021-125189OB-I00, funded by MCIN/AEI/10.13039/501100011033/ by “ERDF A way of making Europe”.

References

[1] M. Arahal, G. Kowal, F. Barrero, and M. Castilla, “Cost function optimization for multi-phase induction machines predictive control,” *Revista Iberoamericana de Automática e Informática Industrial*, vol. 16, no. 1, pp. 48-55, 2019.

[2] C. Lim, E. Levi, M. Jones, N. Rahim, and W.P. Hew, “FCS-MPC-based current control of a five-phase induction motor and its comparison with PI-PWM control,” *IEEE Transactions on Industrial Electronics*, vol. 61, no. 1, pp. 149-163, 2013.

[3] P. de Wit, R. Ortega, and I. Mareels, “Indirect field-oriented control of induction motors is robustly globally stable,” *Automatica*, vol. 32, no. 10, pp. 1393-1402, 1996.

[4] G. Espinosa-Pereza and R. Ortega, “Tuning of PI gains for FOC of induction motors with guaranteed stability,” in *Proceedings of the 23rd International IEEE Conference on Industrial Electronics, Control, and Instrumentation (Cat. No. 97CH36066)*, vol. 2, Nov. 1997, pp. 569-574.

[5] G. Espinosa-Perez, G. Chang, R. Ortega, and E. Mendes, "On field-oriented control of induction motors: Tuning of the PI gains for performance enhancement,” in *Proceedings of the 37th IEEE Conference on Decision and Control (Cat. No. 98CH36171)*, vol. 1, Dec. 1998, pp. 971-976.

[6] A. Bazanella and R. Reginatto, “Robust tuning of the speed loop in indirect field oriented control of induction motors,” *Automatica*, vol. 37, no. 11, pp. 1811-1818, 2001.

[7] R. Ortega, C. Canudas, and S. Seleme, “Nonlinear control of induction motors: Torque tracking with unknown load disturbance,” *IEEE Transactions on Automati Control,* vol. 38, no. 11, pp. 1675-1680, 1993.

[8] M. R. Arahal, M. Berenguel, and E. F. Camacho, "Nonlinear neural model-based predictive control of solar plant," *European IEEE Control Conference*, pp. 985-990, 1997.

[9] R. Marino, S. Peresada, and P. Valigi, " Adaptive input-output linearizing control of induction motors,” *IEEE Transactions on Automatic Control*, vol. 38, no. 2, pp. 208-221, 1993.

[10] F. Rodríguez, M. Berenguel, and M.Arahal, “Feedforward controllers for greenhouse climate control based on physical models,” in *2001 European Control Conference (ECC)*, Sep. 2001, pp. 2158-2163.

[11] G. Ding, X. Wang, and Z. Han, “H^∞ disturbance attenuation control of induction motor,” *International Journal of Adaptive Control and Signal Processing*, vol. 14, no. 2-3, pp. 223-244, 2020.

[12] M. Masiala, B. Vafakhah, J. Salmon, and A. Knight, “Fuzzy self-tuning speed control of an indirect field-oriented control induction motor drive,” *IEEE Transactions on Industry Applications*, vol. 44, no. 6, pp. 1732-1740, 2008.

[13] N. Pham and T. Le, “Novel FOC vector control structure using RBF tuning PI and SM for SPIM drives,” *International Journal of Intelligent Engineering & Systems*, vol. 13, no. 5, pp. 429-440, 2020.

[14] P. Shaija, and A. Daniel, "Optimal tuning of PI controllers for IM drive using GWO and TLBO algorithms," in *2023 Fifth International Conference on Electrical, Computer and Communication Technologies*, Feb. 2023, pp. 1-9.

[15] F. Rodríguez, D. Garrido, R. Núñez, G. Oggier, and G. García, "Feedback linearization contro of a dual active bridge converter feeding a constan power load," *Revista Iberoamericana de Automática e Informática Industrial*, pp. 237-246, 2023.

[16] M. Bermúdez, C. Martín, I. González-Prieto, M. Durán, M. Arahal, and F. Barrero, "Predictive current control in electrical drives: An illustrated review with case examples using a five-phase induction motor drive with distributed windings," *IET Electric Power Applications*, vol. 14, no. 8, pp. 1291-1310, 2020.

[17] P. Gonçalves, S. Cruz, and A. Mendes, "Finite control set model predictive control of six-phase asymmetrica machines -an overview," *Energies*, vol. 12, no. 24, pp. 1-42, 2019.

[18] M.R. Arahal, F. Barrero, M.G. Satué, and M. Bermúdez, "Fast finite-state predictive current control of electric drives," *IEEE Access*, vol. 11, pp. 12821-12828, 2023.

[19] M. Satué, M. Arahal, D. Ramírez, and F. Barrero, "Multi-phase predictive control using two virtual voltage-vector constellations," *Revista Iberoamericana de Automática e Informática Industrial*, vol. 20, no. 4, pp. 347-354, 2023.

[20] H. Zhang, Y. Zhang, Y. Zhu, and X. Wang, "Robust deadbeat predictive current control of induction motor drives with improved steady state performance," *IET Power Electronics*, vol. 16, no. 8, pp. 1271-1454, 2023.

[21] M. Bermúdez, M. Arahal, M. Duran, and I. Gonzalez-Prieto, "Model predictive control of six-phase electric drives including ARX disturbance estimator," *IEEE Transactions on Industrial Electronics*, vol. 68, no. 1, pp. 81-91, 2022.

[22] A. Yepes, O. Lopez, I. Gonzalez-Prieto, M. Duran, and J. Doval-Gandoy, "A comprehensive survey on fault tolerance in multiphase AC drives, part 1: General overview considering multiple fault types," *Machines*, vol. 10, no. 3, pp. 1-134, 2022.

[23] J. Díaz, R. Costa-Castelló, and S. Dormido, "An interactive approach to control systems analysis and design by the root locus technique," *Revista Iberoamericana de Automática e Informática Industrial*, vol. 18, no. 2, pp. 172-188, 2021.

[24] M. Berenguel, M. Arahal, and E. Camacho, "Modelling the free response of a solar plant for predictive control," *Control Engineering Practice*, vol. 6, no. 10, pp. 1257-1266, 1998.

[25] C. Lim, S. Lee and E. Levi, "Continuous control-set model predictive current control of asymmetrical six-phase drives considering system nonidealities," I*EEE Transactions on Industrial Electronics*, vol. 70, no. 8, pp. 7615-7626, 2022.

[26] D. Soto-Marchena, F. Barrero, F. Colodro, M. Arahal, and J. Mora, "On-site calibration of an electric drive: A case study using a multiphase system," *Sensors*, vol. 23, no. 17, pp. 1-15, 2023.

[27] C. Martín, M. Arahal, F. Barrero, and M. Durán, "Multiphase rotor current observers for current predictive control: A five-phase case study," *Control Engineering Practice*, vol. 49, pp. 101-111, 2016.

[28] F. Colodro, J. Mora, F. Barrero, M. Arahal, and J. Martinez-Heredia, "Analysis and simulation of a novel speed estimation method based on oversampling and noise shaping techniques," *Results in Engineering*, vol. 21, pp. 1-9, 2024.

[29] F. Salas, F. Gordillo, J. Aracil, and R. Reginatto, " Codimension-two bifurcations in indirect field oriented control of induction motor drives," *International Journal of Bifurcation and Chaos*, vol. 18, no. 3, pp. 779-792, 2008.